

Anti-inflammatory Sesquiterpenoids from a Sponge-Derived Fungus *Acremonium* sp.

Ping Zhang,^{†,||} Baoquan Bao,^{†,||} Hung The Dang,[†] Jongki Hong,[‡] Hye Ja Lee,[⊥] Eun Sook Yoo,[⊥] Kyung Sook Bae,[§] and Jee H. Jung^{*,†}

College of Pharmacy, Pusan National University, Busan 609-735, Korea, College of Pharmacy, Kyung Hee University, Seoul 130-701, Korea, College of Medicine, Cheju National University, Jeju, 690-756, Korea, and Korea Research Institute of Bioscience and Biotechnology, Daejeon 305-333, Korea

Received October 24, 2008

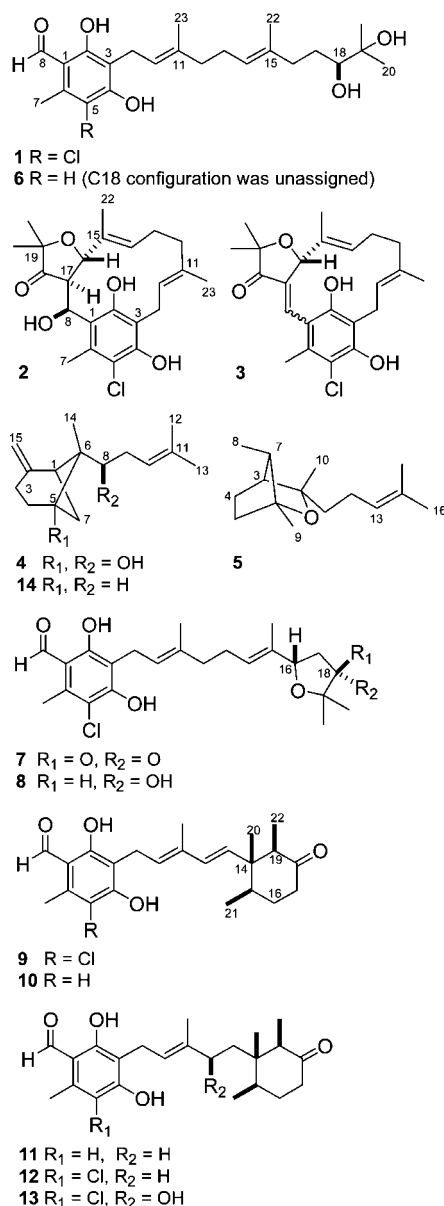
In the course of our search for bioactive metabolites from a sponge-derived fungus *Acremonium* sp., new sesquiterpenoids (**1–4**) were isolated along with known derivatives by bioactivity-guided fractionation. The unique cyclic skeleton of compounds **2** and **3** is unprecedented. The absolute configurations were determined by modified Mosher's method and CD spectroscopy, along with comparison of ¹H and ¹³C NMR spectroscopic data and specific optical rotation values with those reported. The anti-inflammatory activity of the isolated compounds (**1**, **5**, **7–13**) was evaluated by measuring their inhibitory effects on the production of pro-inflammatory mediators (NO, IL-6, and TNF-α) in RAW 264.7 murine macrophage cells. Among the compounds tested, compounds **7** and **9** significantly inhibited the production of NO and TNF-α at the concentration of 100 μM, while compounds **11** and **12** showed selective inhibition of NO production at the same concentration.

Marine microorganisms increasingly draw attention as an important source of bioactive secondary metabolites. In our search for bioactive components from marine microorganisms, the fungal strain *Acremonium* sp., which was isolated from a marine sponge *Stelletta* sp., displayed significant lethality to brine shrimp larvae. Diverse secondary metabolites with varied bioactivities have been reported from the fungal strain of *Acremonium* sp., such as polyketides,^{1,2} terpenoids,^{3,4} steroids,⁴ peptides,^{5–7} and phenolic glycosides.⁸ The EtOAc extract of the culture broth was lethal to the larvae of brine shrimp (*Artemia salina*) with a LD₅₀ value of 72 μg/mL. The EtOAc extract was partitioned between CH₂Cl₂ and water. The CH₂Cl₂ layer was further partitioned between 90% aqueous MeOH and *n*-hexane. The toxicity to the larvae of brine shrimp was found concentrated in the 90% MeOH layer. Further separation and purification of the MeOH layer afforded a series of sesquiterpenoids (**1–13**), including members of the ascochlorin family.

The isolated compounds were characterized as a new chlorinated meros sesquiterpenoid (**1**), cyclic meros sesquiterpenoids (**2** and **3**), sesquiterpenoid **4**, and known sesquiterpenoids (**5–13**, and ilicicolin F). Herein we describe the structure elucidation and the biological evaluation of these compounds.

Results and Discussion

Chlorocylindrocarpol (**1**) was obtained as a yellow, amorphous powder. The FABMS exhibited a characteristic pseudomolecular ion cluster of a monochloro compound at *m/z* 447/449 (3:1) [M + Na]⁺, and the molecular formula was established as C₂₃H₃₃ClO₅ on the basis of the HRFABMS data. The exact mass of the [M + Na]⁺ ion at *m/z* 447.1884 matched well with the expected formula of C₂₃H₃₃ClO₅Na (Δ -3.0 mmu). The molecular formula of **1** suggested that it has seven degrees of unsaturation. The UV spectrum of **1** gave absorption bands at 231 and 290 nm, indicating a high degree of conjugation. The infrared spectrum of **1** showed a broad absorption peak at ν_{max} 3395 cm⁻¹ due to hydroxyl groups and an absorption peak at ν_{max} 1618 cm⁻¹ due to a conjugated



* To whom correspondence should be addressed. Tel: 82-51-510-2803. Fax: 82-51-513-6754. E-mail: jhjung@pusan.ac.kr.

[†] Pusan National University.

[‡] Kyung Hee University.

[⊥] Cheju National University.

[§] Korea Research Institute of Bioscience and Biotechnology.

^{||} These authors equally contributed to this work.

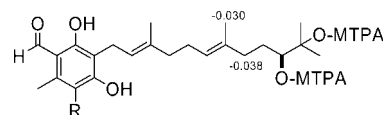
Table 1. ^{13}C and ^1H NMR Data of Compound **1**^a

	δ_{C}	δ_{H}
1	113.5	
2	162.1	
3	114.4	
4	156.6	
5	113.3	
6	137.7	
7	14.4	2.61, s
8	193.2	10.14, s
9	21.9	3.40, d (7.0)
10	121.2	5.20, d (7.0)
11	136.4	
12	39.5	2.02, m
13	26.4	2.10, m
14	124.9	5.16, t (7.5)
15	134.9	
16a	36.7	2.20, m
16b		2.07, m
17a	29.4	1.60, m
17b		1.40, m
18	78.2	3.36, d (10.0)
19	73.1	
20	23.3	1.17, s
21	26.1	1.21, s
22	16.1	1.60, s
23	15.9	1.78, s
2-OH		12.70, s

^a ^{13}C NMR data were measured at 100 MHz in CDCl_3 . ^1H NMR data were measured at 500 MHz in CDCl_3 .

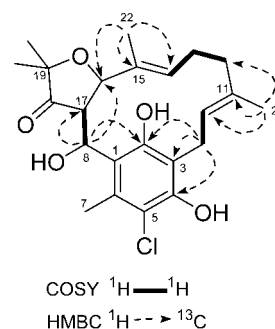
carbonyl group. The spectroscopic properties of **1** were reminiscent of those of cylindrocarpol (**6**).⁹ The main difference from cylindrocarpol (**6**) was the presence of chlorine substitution in **1**. The ^{13}C (Table 1) and DEPT spectra of **1** revealed the presence of five methyls (C-7, 20 to 23), five methylenes (C-9, 12, 13, 16, and 17), an oxymethine (C-18), two olefinic/aromatic methines (C-10 and 14), eight olefinic/aromatic quaternary carbons (C-1, 3, 5, 6, 11, and 15), including two oxygenated quaternary carbons C-2 and 4), an aldehyde (C-8), and an oxygenated quaternary carbon (C-19). In the COSY spectrum, three partial structures having structural fragments C-9–C-10, C-12–C-13–C-14, and C-16–C-17–C-18 were ascertained. The long-range correlations from H-22 (δ_{H} 1.60, 3H) to C-14 (δ_{C} 124.9), C-15 (δ_{C} 134.9), and C-16 (δ_{C} 36.7); H-23 (δ_{H} 1.78, 3H) to C-10 (δ_{C} 121.2), C-11 (δ_{C} 136.4), and C-12 (δ_{C} 39.5); and H-18 (δ_{H} 3.37, 1H) to C-19 (δ_{C} 73.1), C-20 (δ_{C} 23.3), and C-21 (δ_{C} 26.1) established the C₁₅ sesquiterpene skeleton from C-9 to C-23. Six olefinic/aromatic quaternary carbons (C-1 to 6) were responsible for the remaining 4 degrees of unsaturation, indicating the presence of a phenyl ring. The long-range correlations from the chelated hydroxyl proton 2-OH (δ_{H} 12.70) to C-1 (δ_{C} 113.5), C-2 (δ_{C} 162.1), and C-3 (δ_{C} 114.4) and the correlations from H-7 (δ_{H} 2.61, 3H) to C-1, C-5 (δ_{C} 113.3), and C-6 (δ_{C} 137.7) and from H-8 (δ_{H} 10.14, 1H) to C-1 and C-2, along with comparison of chemical shift values with those of known sesquiterpenoids (**7**–**9**, **12**, and **13**), allowed us to establish a 5-chloro-2,4-dihydroxy-6-methylbenzaldehyde-3-yl residue as a partial structure of **1**. The long-range correlations from H-9 (δ_{H} 3.40) to C-2, C-3, and C-4 (δ_{C} 156.6) established the connection between the aliphatic chain and the aromatic ring. The absolute configuration at C-18 was defined by the modified Mosher's method. Negative Δ_{SR} ($\Delta_{\text{S}} - \Delta_{\text{R}}$) values were observed for H-16a (−0.038 ppm) and H-22 (−0.030 ppm), indicating that compound **1** has the 18*S* configuration (Figure 1).

Acremofuranone **A** (**2**) was obtained as a yellow, amorphous powder. The FABMS exhibited a characteristic pseudomolecular ion cluster of a monochloro compound at m/z 419/421 (3:1) [$\text{M} - \text{H}$][−], and the molecular formula was established as C₂₃H₂₆O₅Cl on the basis of the HRFABMS data. The exact mass of the [$\text{M} - \text{H}$][−] ion at m/z 419.1704 matched well with the expected formula of C₂₃H₂₈ClO₅ (Δ +7.9 mmu). The spectroscopic properties of **2** were

**Figure 1.** Δ_{SR} ($\Delta_{\text{S}} - \Delta_{\text{R}}$) values (ppm) for the MTPA esters of compound **1**.**Table 2.** ^{13}C and ^1H NMR Data of Compounds **2** and **3**^a

	2		3	
	δ_{C}	δ_{H}	δ_{C}	δ_{H}
1	115.0		115.5	
2	155.3		152.1	
3	116.7		116.0	
4	148.7		150.1	
5	111.7		113.9	
6	127.9		134.6	
7	14.2 ^b	2.25, s	17.2	2.41, s
8	69.4	5.66, d (2.0)	130.3	7.60, m
9a	21.6	3.56, dd (15.0, 6.5)	22.3	3.82, dd (16.0, 6.5)
9b		2.79, dd (14.0, 8.0)		2.90, dd (16.0, 8.0)
10	125.3	5.82, t (7.5)	125.3	5.76, t (6.5)
11	134.8		134.8	
12	38.2	2.11, m	38.2	2.28, m
13a	26.2	2.29, m	26.2	2.30, m
13b		1.97, m		2.08, m
14	134.3	5.47, d (10.0)	134.3	5.45, br d (10.0)
15	130.4		130.4	
16	79.4	4.90, d (10.0)	79.4	5.20, d (2.0)
17a	54.4	2.68, dd (10.0, 2.0)	54.4	
17b				
18	217.0		217.0	
19	79.1		79.1	
20	20.2	1.24, s	20.2	1.34, s
21	22.9	1.27, s	22.9	1.38, s
22	9.2	1.16, s	9.2	1.15, s
23	14.0 ^b	1.38, s	14.0 ^b	1.29, s
2-OH				5.00, s
4-OH				5.99, s

^a ^{13}C NMR signals of **2** and **3** were assigned by HSQC (or HMBC) experiment in CD_3OD and CDCl_3 , respectively. ^1H NMR data of **2** were measured at 500 MHz in CD_3OD , while those for **3** were measured in CDCl_3 . ^b Assignments with the same superscript in the same column may be interchanged.

**Figure 2.** Key COSY and HMBC correlations of **2**.

reminiscent of those of ascofuranone (**7**).⁵ The main difference from ascofuranone was the replacement of the aldehyde group by a hydroxymethine group, which was connected to C-17 and hence constituted the third ring in **2**. The ^{13}C NMR data (Table 2) of **2** indicated the presence of 23 carbons. In the COSY spectrum, two partial structures having structural fragments C9–C10 and C-12–C-13–C-14 were ascertained (Figure 2). An oxymethine carbon at δ_{C} 79.4 (C-16), another methine carbon at δ_{C} 54.4 (C-17), a ketone carbonyl carbon at δ_{C} 217.0 (C-18), an oxygenated quaternary carbon at δ_{C} 79.1 (C-19), and the geminal dimethyl carbons at δ_{C} 20.2 and 22.9 (C-20 and 21) indicated the presence of a dihydro-2,2-dimethylfuran-3(2*H*)-one-4,5-yl moiety. The long-range correlations from H-22 (δ_{H} 1.16, 3H) to C-14 (δ_{C} 134.3), C-15 (δ_{C}

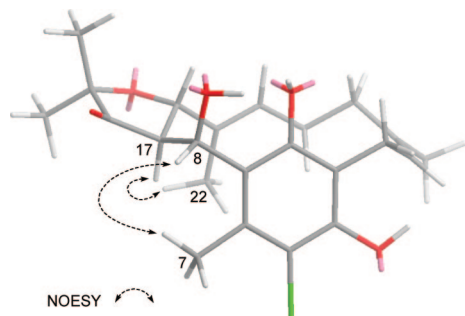
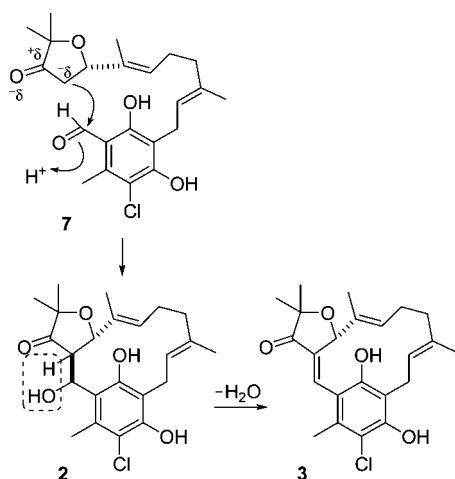


Figure 3. Key NOESY correlations of **2** on the energy-minimized structure.

Scheme 1. Plausible Biogenesis of **2** and **3** by Aldol-Type Condensation



130.4), and C-16 (δ_C 79.4) and from H-23 (δ_H 1.38, 3H) to C-10 (δ_C 125.3), C-11 (δ_C 134.8), and C-12 (δ_C 38.2) (Figure 2) established the linker between C-3 and C-16 and the connection between the aliphatic chain and the furanone moiety. The long-range correlations from H-9a (δ_H 3.56) and H-9b (δ_H 2.79) to C-2 (δ_C 155.3), C-3 (δ_C 116.7), and C-4 (δ_C 148.7) (Figure 2) established the connection between the aliphatic chain and the aromatic ring. The long-range correlations from H-8 (δ_H 5.66) to C-2 (δ_C 155.3), C-16 (δ_C 79.4), and C-17 (δ_C 54.4) (Figure 2) established the connection between the aromatic ring and the furanone moiety. Therefore, compound **2** was assigned as a cyclic derivative of ascofuranone (**7**). The coupling constant between H-16 and H-17 (10.0 Hz) suggested a *trans* configuration at positions C-16 and C-17,¹⁰ which was corroborated by the NOESY correlation between H-17 (δ_H 2.68) and H-22 (δ_H 1.16) (Figure 3). Compound **2** is suspected to be an artifact derived from **7**. However, compound **7** was stable at room temperature in neutral pH. Even after treatment with NaOMe (1 mg/mL) for 18 h at room temperature, no transformation into **2** was observed in the ^1H NMR spectrum (data not shown), arguing against the possibility that **2** would be an artifact. Biogenetically, compound **2** may be derived from **7** by cyclization via an aldol-type condensation (Scheme 1). Accordingly, the same *S*-configuration at C-16 was assumed for **2** and **7**. As the relative configuration at positions C-16 and C-17 was *trans*, the absolute configuration of **2** at C-17 was proposed to be *R*. Due to its cyclic skeleton and bulky substituents, there would not be much freedom for the conformation of the hydroxymethylene moiety (C-8). In addition, a strong NOESY correlation between H-7 (δ_H 2.25) and H-8 was observed, and the estimated dihedral angle between H-8 and H-17 was around 60° , which matched with the small coupling constant (2.0 Hz). Therefore, of the energy-minimized structures, H-8 can be located in the proximity of H-7 only in the case of the *8S*-isomer. However, the absolute configuration at C-8

Table 3. ^{13}C and ^1H NMR Data of Compound **4**^a

	δ_C	δ_H
1	43.5	2.41, ddd, (10.0, 7.0, 1.5)
2	149.7	
3a	26.2	2.62, m
3b		2.33, dd (18.5, 9.5)
4a	32.2	1.94, m
4b		1.76, dt (12.0, 1.5)
5	77.4	
6	53.2	
7a	36.6	2.46, d (7.0)
7b		1.85, d (10.0)
8	75.9	4.32, dd (6.5, 5.5)
9	32.1	2.11, br t (6.5)
10	123.1	5.29, td (8.0, 1.0)
11	133.7	
12	26.0	1.72, br s
13	18.0	1.64, br s
14	11.0	0.82, s
15a	107.9	4.66, dd (1.5, 1.0)
15b		4.59, d (1.5)

^a ^1H and ^{13}C NMR data were measured in CDCl_3 at 500 and 100 MHz, respectively.

could not be independently confirmed by Mosher's method due to the paucity of material.

Acremofuranone B (**3**) was obtained as a yellow, amorphous powder. The FABMS exhibited a characteristic pseudomolecular ion cluster with one chlorine atom at m/z 401/403 (3:1) $[\text{M} - \text{H}]^-$, and the molecular formula was established as $\text{C}_{23}\text{H}_{27}\text{ClO}_4$ on the basis of the HRFABMS data. The exact mass of the $[\text{M} - \text{H}]^-$ ion at m/z 401.1598 matched well with the expected formula of $\text{C}_{23}\text{H}_{26}\text{O}_4\text{Cl}$ (Δ +7.8 mmu). The NMR spectra of **3** were similar to those of acremofuranone A (**2**). The main difference from **2** was observed for the carbons C-8 and C-17. The aliphatic methine (C-17) and oxymethine (C-8) carbons were replaced by vinylic carbons. Therefore, compound **3** was defined as a dehydrated derivative of **2**, and the absolute configuration at C-16 was assumed to be the same as that of **2**. The geometry of the C-8–C-17 double bond remains to be determined, though it is expected to be *E* because the steric energy of the *E*-isomer was much lower than that of the *Z*-isomer in energy minimization using Chemdraw 3D (10 and 28 kcal/mol, respectively).

Dihydroxybergamotene (**4**) was obtained as a colorless, amorphous powder. The FABMS exhibited a pseudomolecular ion at m/z 259 $[\text{M} + \text{Na}]^+$, and the molecular formula was established as $\text{C}_{15}\text{H}_{24}\text{O}_2$ on the basis of the HRFABMS data. The exact mass of the $[\text{M} + \text{Na}]^+$ ion at m/z 259.1661 matched well with the expected formula of $\text{C}_{15}\text{H}_{24}\text{O}_2\text{Na}$ (Δ -1.3 mmu). The spectroscopic properties of **4** were reminiscent of those of β -*trans*-bergamotene (**14**)^{11–14} (Table 3). The main difference from β -bergamotene (**14**) was the presence of two additional hydroxyl groups in **4**. ^{13}C and DEPT NMR data revealed the presence of three methyl carbons (C-12, 13, and 14), five methylene carbons (C-3, 4, 7, 9, and 15), three sp^3 methine carbons (C-1, 8, and 10), and four quaternary carbons (C-2, 5, 6, and 11). These results, together with the molecular formula of **4**, indicated the presence of two exchangeable protons and that **4** should be bicyclic. In the COSY spectrum, structural fragment C-8–C-9–C-10 was ascertained. The long-range correlations from H-9 (δ_H 2.11) to C-11 (δ_C 133.7) and from H-10 (δ_H 5.29) to C-11, C-12 (δ_C 26.0), and C-13 (δ_C 18.0) indicated the presence of a 4-methylpent-3-en-1-ol moiety. The long-range correlations from H-7b (δ_H 1.85) and H-1 (δ_H 2.41) to the vinylic carbon C-2 (δ_C 149.7) and the oxygenated carbon C-5 (δ_C 77.4) and an additional correlation from H-15 (δ_H 4.66 and δ_H 4.59) to C-1 (δ_C 43.5) linked C-1 with C-2 to form a 4-methylene cyclohexanol ring. HMBC correlations of H-1 (δ_H 2.41), H-7b (δ_H 1.85), and H-4b (δ_H 1.76) to the quaternary carbon C-6 (δ_C 53.2), along with an unusually strong four-bond C–H correlation from H-7b (δ_H 1.85) to methyl C-14 (δ_C 11.0), suggested the presence

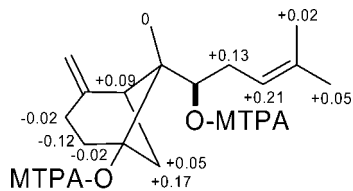


Figure 4. Δ_{SR} ($\Delta_S - \Delta_R$) values for the MTPA esters of compound 4.

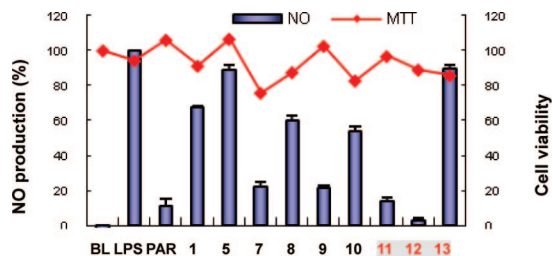


Figure 5. Effects of the compounds (1, 5, and 7–13) on the production of nitric oxide (NO) in LPS-stimulated RAW264.7 cells. RAW264.7 cells were stimulated with LPS (1 $\mu\text{g}/\text{mL}$) alone or in the presence of test samples (100 μM) for 24 h. NO production was determined by Griess reagent methods. Cell viability was determined using the MTT method. The data represent the mean \pm SD of duplicate experiments. PAR, parthenolide (10 μM); BL, blank control.

of a [3,1,1] bicyclic substructure. The long-range correlations from H-8 (δ_{H} 4.32) and H-9 (δ_{H} 2.11) to C-6 established the connectivity between the 4-methylpent-3-en-1-ol moiety and the bicyclic substructure. Therefore, compound 4 was defined as a 5,8-dihydroxy derivative of β -bergamotene (14).

The configuration of 4 was proposed on the basis of NOESY and ^1H NMR data.

A strong NOESY correlation between H-4a (δ_{H} 1.94) and H-14 (δ_{H} 0.82) indicated that they are on the same face, placing H-14 at an axial position of the cyclohexane ring. In addition, the chemical shift of the upfield shifted methyl proton H-14 (δ_{H} 0.82) is similar to those of β -*trans*-bergamotene (δ_{H} 0.70), but different from those of β -*cis*-bergamotene, with the methyl at the equatorial position (δ_{H} 1.20).^{11–14} Therefore, the 6-methyl-endo configuration was assigned. The absolute configuration at C-8 was defined by Mosher's method. Positive Δ_{SR} ($\Delta_S - \Delta_R$) values were observed for H-9 (+0.13 ppm) and H-10 (+0.21 ppm), indicating the 8*R* configuration (Figure 4). However, the absolute configuration of the bicyclic ring remains to be defined.

The structures, including configurations, of the additional sesquiterpenoid derivatives were identified as lignoren (5),¹⁵ cylin-drocarpol (6),⁹ ascofuranone (7),¹⁶ ascofuranol (8),¹⁶ ascochlorin (9),¹⁷ cylindrol B (10),^{9,17} ilicicolin F,⁹ LL-Z 1272 ϵ (11),⁹ ilicicolin C (12),¹⁸ and deacetylchloronectrin (13)¹⁹ on the basis of NMR, CD, and optical activity data.

Compounds 1, 5, and 7–13 were evaluated for their anti-inflammatory activity gauged by their inhibitory effects on the production of major pro-inflammatory mediators (NO, IL-6, and TNF- α) in murine macrophage cells (Figures 5–7). Compounds 7 and 9 showed significant suppressive effects on the production of NO and TNF- α at the concentration of 100 μM , while compounds 11 and 12 were more selective to inhibit NO production.

Experimental Section

General Experimental Procedures. Optical rotations were measured using a JASCO DIP-370 digital polarimeter. CD spectra were recorded using a JASCO J-715 spectropolarimeter (sensitivity 50 mdeg, resolution 0.2 nm). The IR spectrum was recorded using a JASCO FT/IR-410 spectrometer. The UV spectrum was recorded using a Shimadzu

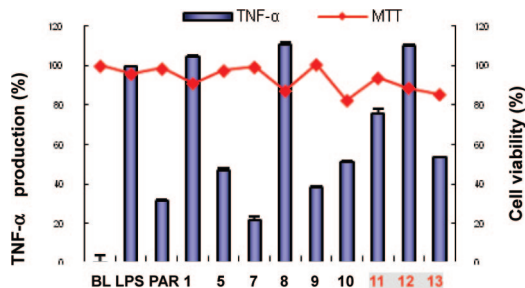


Figure 6. Effects of the compounds (1, 5, and 7–13) on the production of TNF- α in LPS-stimulated RAW264.7 cells. RAW264.7 cells were stimulated with LPS (1 $\mu\text{g}/\text{mL}$) alone or in the presence of test samples (100 μM) for 24 h. TNF- α was determined by ELISA methods. Cell viability was determined using the MTT method. The data represent the mean \pm SD of duplicate experiments. PAR, parthenolide (10 μM); BL, blank control.

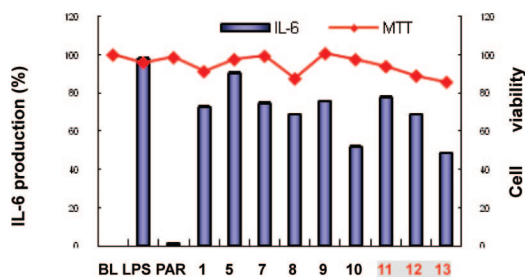


Figure 7. Effects of the compounds (1, 5, and 7–13) on the production of IL-6 in LPS-stimulated RAW264.7 cells. RAW264.7 cells were stimulated with LPS (1 $\mu\text{g}/\text{mL}$) alone or in the presence of test samples (100 μM) for 24 h. IL-6 was determined by ELISA methods. Cell viability was determined using the MTT method. The data represent the mean \pm SD of duplicate experiments. PAR, parthenolide (10 μM); BL, blank control.

UV-1601 UV/visible spectrophotometer. ^1H and ^{13}C NMR spectra were recorded on UNITY 400 and Varian INOVA 500 instruments. Chemical shifts were reported with reference to the respective residual solvent or deuterated solvent peaks (δ_{H} 7.28 and δ_{C} 77.0 for CDCl_3 ; δ_{H} 3.3 and δ_{C} 49.0 for CD_3OD). FABMS data were obtained on a JEOL JMS SX-102A; HPLC was performed with a YMC ODS-H80 column (250 \times 10 mm i.d., 4 μm , 80 \AA) and a Shodex C18 M10E column (250 \times 10 mm i.d., 5 μm , 100 \AA) using a Shodex RI-71 detector.

Fungal Material. The fungal strain *Acremonium* sp. (J05B-1-F-3) was isolated from a sponge *Stelletta* sp. (J05B-1) collected off the coast of Jeju Island, Korea, in October 2005 and was identified by Dr. K. S. Bae. The culture collection is deposited at the Marine Natural Product Laboratory, PNU. The fungus was cultured in malt extract/glucose/peptone (MGP, 20 g of malt extract, 20 g of glucose, and 1 g of peptone in 1 L of artificial seawater at pH 5.5). The fungus was cultured at 24 $^{\circ}\text{C}$ on a shaker platform at 150 rpm for 25 days, in a total of 20 L.

Extraction and Isolation. Culture medium and mycelia were separated by filtration, and then the mycelia were extracted with EtOAc and MeOH, successively. The combined crude extract showed significant toxicity to brine shrimp larvae (LD₅₀ 72.0 $\mu\text{g}/\text{mL}$). The combined crude extract (3.56 g) was partitioned between CH_2Cl_2 and water. The toxicity to brine shrimp larvae was concentrated in the CH_2Cl_2 layer (LD₅₀ 17.0 $\mu\text{g}/\text{mL}$). The CH_2Cl_2 layer was further partitioned between aqueous MeOH and *n*-hexane. The MeOH layer showed significant toxicity to brine shrimp larvae (LD₅₀ 8.0 $\mu\text{g}/\text{mL}$). The MeOH layer residue was subjected to reversed-phase flash column chromatography (YMC gel ODS-A, 60 \AA , 230 mesh) using stepwise elution with a solvent system of 30–100% MeOH/ H_2O to afford 10 fractions. Fraction 7 (101.0 mg), one of the bioactive fractions (LD₅₀ 26.0 $\mu\text{g}/\text{mL}$, brine shrimp assay), was subjected to RP HPLC eluting with 75% MeOH to afford compounds 1 (2.7 mg), 4 (3.2 mg), 7 (8.0 mg), 8 (4.0 mg), 9 (57.8 mg), 10 (3.8 mg), ilicicolin F (3.6 mg), and 11 (13.9 mg). Compounds 2 (0.7 mg), 3 (0.8 mg), and 6 (1.2 mg) were obtained by separation of the bioactive fraction 6 (210 mg, LD₅₀ 100 $\mu\text{g}/\text{mL}$) on a reversed-phase HPLC

eluting with 70% MeOH. Compounds **5** (10 mg) and **13** (12.5 mg) were obtained by separation of another bioactive fraction, 5 (124.0 mg, LD₅₀ 150 µg/mL), on a reversed-phase HPLC eluting with 65% MeOH. Fraction 8 (323 mg), the most toxic fraction (LD₅₀ 2 µg/mL, brine shrimp assay), was subjected to reversed-phase HPLC eluting with 85% MeOH to afford compounds **11** (13.9 mg) and **12** (2.2 mg).

Chlorocylindrocarpol (1): yellow, amorphous powder; $[\alpha]_D^{25} +5.0$ (*c* 0.27, MeOH); UV (MeOH) λ_{\max} (log ϵ) 231 (4.36), 290 (4.32), 339 (4.02) nm; IR ν_{\max} 3395, 2924, 1619, 1456, 1419, 1375, 1283, 1249, 1159, 1109, 1076 cm⁻¹; ¹H NMR data (CDCl₃, 500 MHz), see Table 1; ¹³C NMR data (CDCl₃, 125 MHz), see Table 1; HRFABMS *m/z* 447.1884 [M + Na]⁺ (calcd for C₂₃H₃₃ClO₅Na, 447.1914).

Acremofuranone A (2): yellow, amorphous powder; $[\alpha]_D^{25} +5.0$ (*c* 0.06, MeOH); UV (MeOH) λ_{\max} (log ϵ) 223.5 (3.81), 288 (3.29), 339 (2.77) nm; IR ν_{\max} 3275, 2925, 2855, 1753, 1614, 1583, 1448, 1422, 1377, 1281, 1247, 1171, 1089, 1063, 1029, 982 cm⁻¹; ¹H NMR data (CD₃OD, 500 MHz), see Table 2; ¹³C NMR data (assigned by HSQC or HMBC experiment in CD₃OD), see Table 2; HRFABMS *m/z* 419.1704 [M - H]⁻ (calcd for C₂₃H₂₈ClO₅, 419.1625).

Acremofuranone B (3): yellow, amorphous powder; $[\alpha]_D^{25} +5.0$ (*c* 0.08, MeOH); UV (MeOH) λ_{\max} (log ϵ) 219 (3.74), 263 (3.48), 327 (3.47) nm; IR ν_{\max} 3421, 2925, 2855, 1719, 1624, 1590, 1455, 1375, 1263, 1167, 1139, 1094, 1026, 988 cm⁻¹; ¹H NMR data (CDCl₃, 500 MHz), see Table 2; ¹³C NMR data (assigned by HSQC or HMBC experiment in CDCl₃), see Table 2; HRFABMS *m/z* 401.1598 [M - H]⁻ (calcd for C₂₃H₂₆ClO₄, 401.1520).

Dihydroxybergamotene (4): colorless, amorphous powder; $[\alpha]_D^{20} -14.4$ (*c* 0.30, MeOH); UV (MeOH) λ_{\max} (log ϵ) 216 (2.87), 292 (2.49), 336 (2.40) nm; IR ν_{\max} 3347, 2929, 1644, 1452, 1434, 1377, 1329, 1285, 1239, 1186, 1126, 1062, 875 cm⁻¹; ¹H NMR data (CDCl₃, 500 MHz), and ¹³C NMR data (CDCl₃, 125 MHz), see Table 3; HRFABMS *m/z* 259.1661 [M + Na]⁺ (calcd for C₁₅H₂₄O₂Na, 259.1674).

Lignoren (5): $[\alpha]_D^{20} -20.4$ (*c* 0.57, MeOH). In the NOESY spectrum of **5**, the correlation from H-8 (δ_H 1.04) to H-4a (δ_H 1.85) and H-5a (δ_H 1.61) and from H-10 to H-4 (δ_H 1.55) corroborated the depicted relative configuration of **5**, which was not defined in the original reference.¹⁵

Ascofuranone (7): $[\alpha]_D^{25} -28.8$ (*c* 0.80, MeOH), natural ascofuranone (-50.0, *c* 1.0, MeOH),¹⁶ synthetic (*S*)-ascofuranone (-37.0, *c* 0.13, MeOH).²⁰

Ascofuranone (8): $[\alpha]_D^{25} -5.7$ (*c* 0.40, MeOH), natural ascofuranone (-7.0, *c* 1.0, MeOH),¹⁶ synthetic (14*S*,16*S*)-ascofuranol (-3.1, *c* 0.37, MeOH), synthetic (14*R*,16*R*)-ascofuranol (+3.2, *c* 0.54, MeOH).²⁰

Asochlorin (9):¹⁷ $[\alpha]_D^{25} -35.8$ (*c* 0.50, MeOH); CD (*c* 3.5 × 10⁻³ M) $\Delta\epsilon$ (nm) -5.95 (291.8).

Cylindrol B (10):⁹ $[\alpha]_D^{25} -27.8$ (*c* 0.38, MeOH); CD (*c* 3.4 × 10⁻³ M) $\Delta\epsilon$ (nm) -3.83 (289.8).

Illicolin F:⁹ $[\alpha]_D^{25} +5.4$ (*c* 0.35, MeOH); CD (*c* 3.5 × 10⁻³ M) $\Delta\epsilon$ (nm) -2.83 (291.2).

LL-Z1272 ϵ (11):⁹ $[\alpha]_D^{25} +3.86$ (*c* 0.50, MeOH); CD (*c* 3.6 × 10⁻³ M) $\Delta\epsilon$ (nm) -2.24 (287.8).

Illicolin C (12):¹⁸ $[\alpha]_D^{25} +5.24$ (*c* 0.20, MeOH); CD (*c* 3.5 × 10⁻³ M) $\Delta\epsilon$ (nm) -2.47 (286.8).

Deacetylchloronectrin (13):¹⁹ $[\alpha]_D^{25} +15.6$ (*c* 0.50, MeOH); CD (*c* 2.7 × 10⁻³ M) $\Delta\epsilon$ (nm) -1.30 (288.2), +1.84 (242.8 nm).

Preparation of the (R)- and (S)-MTPA Esters of 1. Two portions (0.4 and 0.7 mg, respectively) of compound **1** were treated overnight with (*S*)-(+)- and (*R*)-(-)- α -methoxy- α -(trifluoromethyl)phenylacetyl chloride (1 µL) in CDCl₃ (0.5 mL)/C₅D₅N (4 µL) at room temperature to afford the (*R*)- and (*S*)-MTPA esters, respectively (**1r** and **1s**, respectively).

(*R*)-MTPA esters (**1r**): ¹H NMR (CD₃OD, 500 MHz) 10.40 (1H, s, H-8), 5.22 (1H, m, H-10), 5.19 (1H, m, H-14), 3.57 (2H, m, H-9), 4.24 (1H, m, H-18), 2.72 (3H, s, H-7), 2.35 (2H, m, 13), 2.257 (1H, m, H-16a), 2.173 (1H, m, H-16b), 2.14 (2H, m, 12), 1.968 (3H, s, H-22), 1.63–1.59 (1H, m, H-17a), 1.58 (3H, s, H-23), 1.47–1.43 (1H, m, H-17b), 1.15 (3H, s, H-21), 1.12 (3H, s, H-20).

(*S*)-MTPA esters (**1s**): ¹H NMR (CD₃OD, 500 MHz) 10.40 (1H, s, H-8), 5.35 (1H, m, H-10), 5.19 (1H, m, H-14), 3.57 (2H, m, H-9), 4.24 (1H, m, H-18), 2.72 (3H, s, H-7), 2.35 (2H, m, 13), 2.219 (1H, m, H-16a), 2.172 (1H, m, H-16b), 2.14 (2H, m, 12), 1.938 (3H, s, H-22), 1.63–1.59 (1H, m, H-17a), 1.58 (3H, s, H-23), 1.47–1.43 (1H, m, H-17b), 1.15 (3H, s, H-21), 1.12 (3H, s, H-20).

Preparation of the (R)- and (S)-bisMTPA Esters of 4. Two portions (0.4 and 0.5 mg, respectively) of compound **1** were treated

overnight with (*S*)-(-) and (*R*)-(+)- α -methoxy- α -(trifluoromethyl)phenylacetyl chloride (1 µL) in CDCl₃ (0.5 mL)/C₅D₅N (4 µL) at room temperature to afford the (*R*)- and (*S*)-bisMTPA esters, respectively (**4r** and **4s**, respectively).

(*R*)-MTPA esters (**4r**): ¹H NMR (CDCl₃, 500 MHz) 5.03 (1H, t, H-10), 4.73 (1H, s, H-15a), 4.64 (1H, s, H-15b), 3.69 (1H, dd, H-8), 2.72 (1H, m, H-3a), 2.48 (1H, d, H-7a), 2.53 (1H, d, H-1), 2.44 (1H, m, H-4a), 2.42 (1H, m, H-7b), 2.40 (1H, m, H-3b), 2.04 (1H, t, H-4b), 1.97 (2H, br t, H-9), 1.71 (1H, s, H-12), 1.57 (1H, s, H-13), 0.85 (1H, s, H-14).

(*S*)-MTPA esters (**4s**): EIMS *m/z* 640 [M]⁺; ¹H NMR (CDCl₃, 500 MHz) 5.24 (1H, t, H-10), 4.74 (1H, s, H-15a), 4.66 (1H, s, H-15b), 4.17 (1H, t, H-8), 2.72 (1H, m, H-3a), 2.62 (1H, t, H-1), 2.65 (1H, d, H-7a), 2.47 (1H, d, H-7b), 2.38 (1H, m, H-3b), 2.42 (1H, m, H-4a), 2.10 (2H, br t, H-9), 1.92 (1H, m, H-4b), 1.73 (1H, s, H-12), 1.62 (1H, s, H-13), 0.85 (1H, s, H-14).

Cytotoxicity Assay. Cytotoxic effects were evaluated in cells cultured for 24 h using the MTT (3-[4,5-dimethylthiazol-2-yl]-2,5-diphenyl tetrazolium bromide) assay. MTT was added to cells, and after 4 h, cultures were removed from the incubator and the formazan crystals were dissolved by adding DMSO. Metabolic activity was quantified by measuring light absorbance at 540 nm.

Nitrite Assay. The production of nitric oxide (NO) was measured, as previously described by Ryu et al.,²² by using the Griess reagent (Sigma, MO). Briefly, the RAW 264.7 cells were stimulated with LPS (1 µg/mL), and 100 µL of the supernatant was mixed with 100 µL of the Griess reagent (0.1% naphthylene diamine dihydrochloride, 1% sulfanilamide, 2.5% H₃PO₄). This mixture was incubated for 10 min at room temperature (light protected). Absorbance at 540 nm was measured using an ELISA reader (Amersham Pharmacia Biotech, UK), and the results were compared against a calibration curve using sodium nitrite as the standard.

Measurement of the Production of Pro-inflammatory Cytokines (IL-6 and TNF- α). The inhibitory effects of the isolated compounds on IL-6 and TNF- α production were determined by the method previously described.²³ The samples were dissolved with EtOH and diluted with DMEM. The final concentration of chemical solvents did not exceed 0.1% in the culture medium. At these conditions, none of the solubilized solvents altered IL-6 and TNF- α production in RAW 264.7 cells. Before stimulation with LPS (1 µg/mL) and test materials, RAW 264.7 cells were incubated for 18 h in 24-well plates under the same conditions. Lipopolysaccharide (LPS) and the test materials were then added to the cultured cells. The medium was used for IL-6 and TNF- α assay using mouse ELISA kits (R & D Systems Inc., MN).

Acknowledgment. The study was supported by a grant from Marine Biotechnology Program funded by Ministry of Land, Transport, and Maritime Affairs, Korea.

Supporting Information Available: ¹H and ¹³C NMR data of compounds **5**–**13**. This material is available free of charge via the Internet at <http://pubs.acs.org>.

References and Notes

- Pontius, A.; Mohamed, I.; Krick, A.; Kehraus, S.; Konig, G. M. *J. Nat. Prod.* **2008**, *71*, 272–274.
- Agatsuma, T.; Akama, T.; Nara, S.; Matsumiya, S.; Nakai, R.; Ogawa, H.; Otaki, S.; Ikeda, S.; Saitoh, Y.; Kanda, Y. *Org. Lett.* **2002**, *4*, 4387–4390.
- Cagnoli-Bellavita, N.; Ceccherelli, P.; Fringuelli, R.; Ribaldi, M. *Phytochemistry* **1975**, *14*, 807.
- Ondeyka, J. G.; Jayasuriya, H.; Herath, K. B.; Guan, Z.; Schulman, M.; Collado, J.; Dombrowski, A. W.; Kwon, S. S.; McCallum, C.; Sharma, N.; MacNaul, K.; Hayes, N.; Menke, J. G.; Singh, S. B. *J. Antibiot.* **2005**, *58*, 559–565.
- Ratnayake, R.; Fremlin, L. J.; Lacey, E.; Gill, J. H.; Capon, R. J. *J. Nat. Prod.* **2008**, *71*, 403–408.
- Boot, C. M.; Amagata, T.; Tenney, K.; Compton, J. E.; Pietraszkiewicz, H.; Valeriote, F.; Crews, P. *Tetrahedron* **2007**, *63*, 9903–9914.
- Boot, C. M.; Tenney, K.; Valeriote, F. A.; Crews, P. *J. Nat. Prod.* **2006**, *69*, 83–92.
- Bunyapaiboonsri, T.; Yoiprommarat, S.; Khonsanit, A.; Komwijit, S. *J. Nat. Prod.* **2008**, *71*, 891–894.
- Singh, S. B.; Ball, R. G.; Bills, G. F.; Cascales, C.; Gibbs, J. B.; Goetz, M. A.; Hoogsteen, K.; Jenkins, R. G.; Liesch, J. M.; Lingham, R. B.; Silverman, K. C.; Zink, D. L. *J. Org. Chem.* **1996**, *61*, 7727–7737.
- Angle, S. R.; Choi, I.; Tham, F. S. *J. Org. Chem.* **2008**, *73*, 6268–6278.

- (11) Corey, E. J.; Cane, D. E.; Libit, L. *J. Am. Chem. Soc.* **1971**, *93*, 7016–7021.
- (12) Cane, D. E.; King, G. G. S. *Tetrahedron Lett.* **1976**, *51*, 4737–4740.
- (13) Kulkarni, Y. S.; Niwa, M.; Ron, E.; Snider, B. B. *J. Org. Chem.* **1987**, *52*, 1568–1576.
- (14) Cane, D. E.; McIlwaine, D. B.; Oliver, J. S. *J. Am. Chem. Soc.* **1990**, *112*, 1285–1286.
- (15) Berg, A.; Wangun, H. V. K.; Nkengfack, A. E.; Schlegel, B. *J. Basic Microbiol.* **2004**, *44*, 317–319.
- (16) Sasaki, H.; Hosokawa, T.; Sawada, M.; Ando, K. *J. Antibiot.* **1973**, *26*, 676–680.
- (17) (a) Tamura, G.; Suzuki, S.; Takatsuki, A.; Ando, K.; Arima, K. *J. Antibiot.* **1968**, *21*, 539–544. (b) Dudley, G. B.; Takaki, K. S.; Cha, D.; Danheiser, R. L. *Org. Lett.* **2000**, *2*, 3407–3410.
- (18) Hayakawa, S.; Minato, H.; Katagiri, K. *J. Antibiot.* **1971**, *24*, 653–654.
- (19) Aldridge, D. C.; Borrow, A.; Foster, R. G.; Large, M. S.; Spencer, H.; Turner, W. B. *J. Chem. Soc., Perkin Trans. 1* **1972**, 2136–2141.
- (20) Mori, K.; Takechi, S. *Tetrahedron* **1985**, *41*, 3049–3062.
- (21) Takamatsu, S.; Rho, M. C.; Masuma, R.; Hayashi, M.; Komiyama, K.; Tanaka, H.; Omura, S. *Chem. Pharm. Bull.* **1994**, *42*, 953–956.
- (22) Ryu, S. Y.; Oak, M. H.; Yoon, S. K.; Cho, D. I.; Yoo, G. S. *Planta Med.* **2000**, *66*, 358–360.
- (23) Cho, J. Y.; Baik, K. U.; Jung, J. H.; Park, M. H. *Eur. J. Pharmacol.* **2000**, *398*, 399–407.

NP8006793